Evaluation of some thiadiazole derivatives as acid corrosion inhibitors for carbon steel in aqueous solutions

A.S. Fouda[*], K. Shalabi, R. Ezzat

Chemistry Department, Faculty of Science, Mansoura University, Mansoura-35516, Egypt,

Abstract

Inhibition of C-steel corrosion by some thiadiazole derivatives in 1 M HCl was investigated by weight loss, potentiodynamic polarization, electrochemical impedance spectroscopy (EIS) and electrochemical frequency modulation (EFM) measurements. The inhibition efficiency increased with increase in inhibitor concentration but deceased with rise in temperature. The thermodynamic parameters of corrosion and adsorption processes were determined and discussed. The adsorption of these inhibitors was found to obey Langmuir adsorption isotherm. The results obtained from the three different techniques were in good agreement. Quantum structure-activity relationships have been used to study the effect of molecular structure on inhibition efficiency of the inhibitors. The surface morphology of carbon steel sample was investigated by scanning electron microscopy (SEM) and energy dispersive X-ray (EDX) studies

Keywords: Corrosion inhibition; C-steel; HCl; thiadiazole derivatives

1. Introduction

Corrosion and corrosion inhibition of iron andiron alloys, in general, and steel, in particular, have received a great attention in different media [1– 5] with and without various types of inhibitors. The corrosion inhibition of C-steel becomes of such interest because it is widely used as a constructional material in many industries and this is due to its excellent mechanical properties and low cost. Acid solutions are generally used for the removal of undesirable scale and rust in several petroleum processes. Inhibitors are used in this process to control metal dissolution. Most of the well-known acid inhibitors are organic compounds containing O, S, and /or N atoms [6-9]. The corrosion inhibition efficiency of organic compounds is related to their adsorption properties. Adsorption depends on the nature and the state of the metal surface, on the type of corrosive medium and on the chemical structure ofthe inhibitor [10]. Studies report that the adsorption of the organic inhibitors mainly depends on some physico-chemical properties of the molecule related to its functional group, to the possible steric effects and electronic density of donor atoms; adsorption is also supposed to depend on the possible interaction of π-orbitals of the inhibitor with d-orbitals of the surface atoms, which induce greater adsorption of the inhibitor molecules onto the surface of C-steel, leading to the formation of corrosion protecting film [11,12].Quantum chemical calculations have been widely used to study the reaction mechanism and to interpret the experimental results as well as to solve chemical ambiguities. This is a useful approach to investigate the reaction mechanism of the inhibitors molecules and the metal surface. The structural and electronic parameters of the inhibitors molecules can be obtained by means of theoretical calculations using the computational methodologies of quantum chemistry [13]. Sherif et al investigated the influence of 2-amino-5-ethylthio-1,3,4-thiadiazole(AETD) on copper corrosion in aerated HCl solution [14] as well as the influence of 2-amino-5-ethylthio-1,3,4-thiadiazole (AETD) [15], 2-amino-5-ethyl-1,3,4-thiadiazole (AETDA) [16] and 5-(phenyl)-4H-1,2,4-triazole-3-thiole (PTAT) [17] in NaCl solution. Vastag [18] investigated thiazole derivatives: 5-benzylidene-2,4-dioxotetrahydro-1,3-thiazole (BDT); 5-(4'-isopropylbenzylidene)-2,4-dioxotetrahydro-1,3-thiazole (IPBDT); 5-(3'-thenylidene)-2,4-dioxotetrahydro-1,3-thiazole (TDT) and 5-(3',4'-dimetoxy benzylidene)-2,4-dioxotetrahydro-1,3-thiazole (MBDT) as copper corrosion inhibitors in 0.1M sodium sulphate solution, pH=2.94.
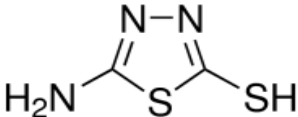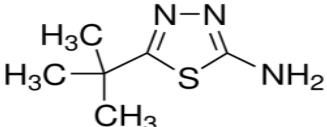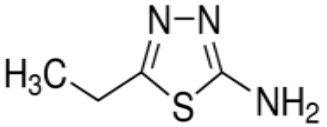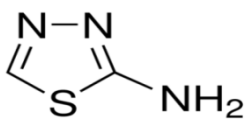
The present work was designed to study the corrosion inhibition of C-steel in 1M HCl solutions by some thiadiazole derivatives as corrosion inhibitors using chemical and electrochemical techniques, also, to compare the experimental results with the theoretical ones.

2. Experimental Methods

2.2. Materials and Solutions

The carbon steel used having composition (weight %): C 0.2; Mn 0.9; P 0.007; Si 0.002 % and the rest Fe.The experimental measurements were carried out in 0.1 M HCl solution in the absence and presence of various concentrations of thiadiazole derivatives.The chemical structure of thiadiazole derivatives is given in Table 1. The thiadiazole derivatives presented in Table 1 were purchased from Oxford Laboratory Reagent, Mumbai, India.The concentrations of inhibitors employed were varied from 5x 10^{-6} M to 21 x 10^{-6} M. For each experiment, a freshly prepared solution was used.

Table 1: Chemical structures, names, molecular weights and molecular formulas of investigated compounds

Inhibitor	Structures	Names	Molecular weights and Molecular Formulas
1		5-Amino-1,3,4-thiadiazole-2-thiol	133.20 $C_2H_3N_3S_2$
2		2-Amino-5-tert-butyl-1,3,4-thiadiazole	157.24 $C_6H_{11}N_3S$
3		2-amino-5-ethyl-1,3,4-thiadiazole	129.18 $C_4H_7N_3S$
4		2-Amino-1,3,4-thiadiazole	101.13 $C_2H_3N_3S$

2.3 Weight Loss Measurements

Carbon steel sheets of 20 x 20 x 2 mm were abraded with different grades of emery paper up to 1200 grit and then washed with bidistilled water and acetone. After weighing accurately, the specimens were immersed in 100ml HCl solution with and without addition of different concentrations of inhibitors. After 3 hrs, the specimens were taken out, washed, dried, and weighed accurately. The average weight loss of the three parallel C- steel sheets could be obtained at required temperature. The inhibition efficiency (IE) and the degree of surface coverage (θ) of the investigated inhibitors on the corrosion of C-steel were calculated as follows [19]:

$$IE \% = \theta \times 100 = [1- (W / W°)] \times 100 \qquad (1)$$

Where W° and W are the values of the average weight loss without and with addition of the inhibitor, respectively.

2.4 Electrochemical Measurements

2.4.1 Potentiodynamic Polarization Measurements

Polarization experiments were carried out in a conventional three-electrode cell with platinum gauze as the auxiliary electrode and a saturated calomel electrode (SCE) coupled to a fine Luggin capillary as reference electrode. The working electrode was in the form of a square cut from carbon steel sheet of equal composition embedded in epoxy resin of polytetrafluoroethylene so that the flat surface area was 1 cm^2. Prior to each measurement, the electrode surface was pretreated in the same manner as the weight loss experiments. Before measurements, the electrode was immersed in solution for 30 min. until a steady state was reached. The potential was started from - 600 to + 400 mV vs. open circuit potential (E$_{ocp}$). All experiments were carried out in freshly prepared solutions at 25°C and results were always repeated at

least threetimes to check the reproducibility.Then i_{corr} was used for the calculation of inhibition efficiency and surface coverage (θ) as below:

$$\%IE = \theta \times 100 = [1-(i_{corr}/i°_{corr})] \times 100 \quad (2)$$

where $i°_{corr}$ and i_{corr} are corrosion current densities in the absence and presence of inhibitor, respectively.

2.4.2. Electrochemical Impedance Spectroscopy Measurements
Impedance measurements were carried out using AC signals of 5 mV peak to peak amplitude at the open circuit potential in the frequency range of 100 kHz to 0.1 Hz. All impedance data were fitted to appropriate equivalent circuit using the Gamry Echem Analyst software version 6.03.

2.4.3. Electrochemical Frequency Modulation Measurements
EFM experiments were performed with applying potential perturbation signal with amplitude 10 mV with two sine waves of 2 and 5 Hz. The choice for the frequencies of 2 and 5 Hz was based on three arguments [20-22].The larger peaks were used to calculate the corrosion current density (i_{corr}), the Tafel slopes (β_c and β_a) and the causality factors CF-2 and CF-3[23].The electrode potential was allowed to stabilize for 30 min before starting the measurements. All the experiments were conducted at $25 \pm 1°C$. Measurements were performed using Gamry Instrument Potentiostat/ Galvanostat/ ZRA (PCI4-G750). This includes a Gamry framework system v 6.03 Gamry applications include DC105 software for DC corrosion measurements, EIS300 software for electrochemical impedance spectroscopy measurements and EFM140 for electrochemical frequency modulation measurements along with a computer for collecting data. Echem analyst v 6.03 software was used for plotting, graphing, and fitting data.

2.5 Quantum Chemical Calculations
The molecular structures of the investigated compounds were optimized initially with PM3 semi empirical method so as to speed up the calculations. All the quantum chemical calculations were performed with Material studio V. 6.0.

2.6 Scanning Electron Microscopy Measurements (SEM,EDX)
The electrode surface of C-steel was examined by Scanning Electron Microscope – type JOEL 840, Japan before and after immersion in 1 M HCl test solution in the absence and in presence of the optimum concentrations of the investigated inhibitors at 25°C, for 1 day immersion time. The specimens were washed gently with bidistilled water, then dried carefully and examined without any further treatments.

3. Results and Discussion
3.1 Chemical Method (Weight Loss Measurements)
Weight-loss of C-steel was determined, at various time intervals, in the absence and presence of different concentrations of investigated thiadiazole derivatives. The obtained weight-loss time curves are represented in Figure 1 for inhibitor (1), the most effective one. Similar curves were obtained for other inhibitors (not shown). The inhibition efficiency was found to be dependent on the inhibitor concentrations and temperature. The curves obtained in the presence of inhibitors fall significantly below that of free acid. In all cases, the increase in the inhibitor concentration was accompanied by a decrease in weight-loss and an increase in the % inhibition. These results lead to the conclusion that these investigated compounds are fairly efficient as inhibitors for C-steel dissolution in hydrochloric acid solution. In order to get a comparative view, the variation of the % inhibition (IE) of the four inhibitors with their molar concentrations was calculated. The values obtained are summarized in Table 2. Careful inspection of these results showed that, at the same inhibitor concentration, the order of inhibition efficiencies is as follows:1>2>3>4(Figure 2).

3.2 Effect of Temperature
The effect of temperature on the corrosion rate of C-steel in 1M HCl and in presence of different inhibitors concentrations was studied in the temperature range of 298–318K using weight loss measurements. As the temperature increases, the rate of corrosion increases and the inhibition efficiency of the additives decreases asshownin Table 3 for investigated inhibitors. The adsorption behavior of inhibitors on HCl surface occurs through physical adsorption.
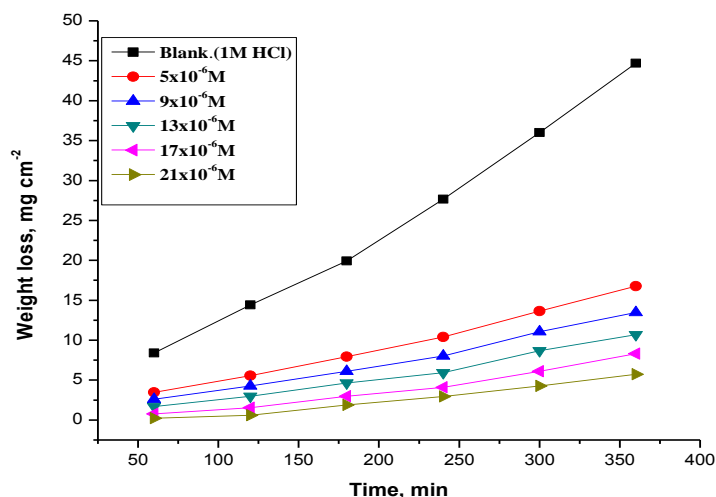
Figure 1. Weight loss-time curves for the corrosion of C-steel in 1 M HCl in the absence and presence of different concentrations of inhibitor (1) at 25 °C
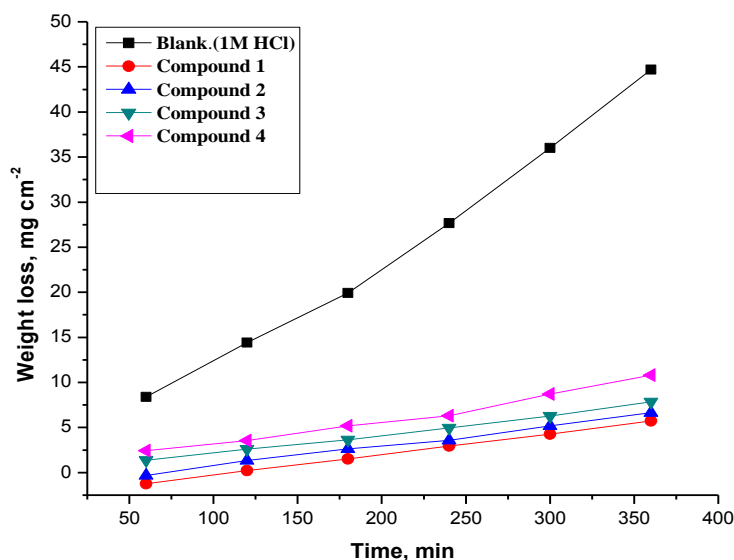
Figure 2. Weight loss-time curve for C-steel corrosion in the presence and absence of 21 x 10^{-6} M of different compounds at 25°C

Table 2. Values of inhibition efficiencies (%IE) and surface coverage (θ) of inhibitors for the corrosion of C-steel in 1 M HCl from weight-loss measurements at different concentrations and at 25°C

[inh]x10^{-6}M	1		2		3		4	
	Θ	% IE	Θ	% IE	Θ	% IE	Θ	% IE
5	0.624	62.4	0.574	57.4	0.523	52.3	0.436	43.6
9	0.711	71.1	0.656	65.6	0.591	59.1	0.523	52.3
13	0.786	78.6	0.740	74.0	0.664	66.4	0.601	60.1
17	0.852	85.2	0.805	80.5	0.732	73.2	0.682	68.2
21	0.893	89.3	0.870	87.0	0.821	82.1	0.772	77.2

Table 3. Inhibition efficiency (%IE) of the thiadiazole derivatives at different concentrations after testing C-steel in 1 M HCl solution at different temperatures

Inhibitor	Concentration, M.	%IE				
		25˚C	30˚C	35˚C	40˚C	45˚C
1	5 x 10⁻⁶	62.4	60.1	58.4	55.8	53.8
	9 x 10⁻⁶	71.1	68.3	66.2	63.1	60.9
	13 x 10⁻⁶	78.6	75.2	72.6	68.3	65.0
	17 x 10⁻⁶	85.2	81.1	78.0	74.7	71.2
	21 x 10⁻⁶	89.3	86.3	83.3	79.1	77.1
2	5 x 10⁻⁶	57.4	55.9	52.2	51.2	49.9
	9 x 10⁻⁶	65.6	62.4	60.3	59.3	56.1
	13 x 10⁻⁶	74.02	69.1	66.4	63.2	60.2
	17 x 10⁻⁶	80.5	77.3	74.6	70.0	66.2
	21 x 10⁻⁶	87.0	82.4	79.2	78.1	74.9
3	5 x 10⁻⁶	52.3	50.4	46.9	45.8	42.7
	9 x 10⁻⁶	59.1	56.1	53.3	52.4	50.3
	13 x 10⁻⁶	66.4	62.2	61.4	58.1	57.2
	17 x 10⁻⁶	73.2	70.4	68.3	66.4	64.0
	21 x 10⁻⁶	82.1	77.3	74.6	72.6	70.6
4	5 x 10⁻⁶	43.6	42.2	39.8	37.3	34.8
	9 x 10⁻⁶	52.3	49.4	47.3	43.1	41.3
	13 x 10⁻⁶	60.1	57.2	55.2	52.7	50.2
	17 x 10⁻⁶	68.2	64.1	62.5	60.1	59.4
	21 x 10⁻⁶	77.2	72.1	69.7	67.0	65.5

3.3 Adsorption isotherms

One of the most convenient ways of expressing adsorption quantitatively is by deriving the adsorption isotherm that characterizes the metal/inhibitor/ environment system.Various adsorption isotherms were applied to fit ϴ values but the best fit was found to obey Langmuir adsorption isotherm which are represented in Figure 3 for investigated inhibitors, Langmuir adsorption isotherm may be expressed by:

$$C/\Theta = 1/K_{ads} + C \qquad (3)$$

where C is the concentration (mol L^{-1}) of the inhibitor in the bulk electrolyte, ϴ is the degree of surface coverage(ϴ=% IE/100), K_{ads} is the adsorption equilibrium constant. A plot of C versus C/ϴ should give straight line.In order to get a comparative view, the variation of the adsorption equilibrium constant (K_{ads}) of the inhibitors with their molar concentrations was calculated. The experimental data give good curves fitting for the applied adsorption isotherm as the correlation coefficients (R^2) were in the range (0.943- 0.999). The values obtained are given in Table 4.These results confirm the assumption that, these compounds are adsorbed on the metal surface through the lone pairs of electrons of (N, S) atoms. The extent of inhibition is directly related to the performance of adsorption layer which is a sensitive function of the molecular structure. The equilibrium constant of adsorption K_{ads} obtained from the intercepts of Langmuir adsorption isotherm is related to the free energy of adsorption ΔG° ads as follows:

$$K_{ads}=1/55.5 \exp [-\Delta G°_{ads}] / RT] \qquad (4)$$

where, 55.5 is the molar concentration of water in the solution in M^{-1}.

Plot of ($\Delta G°_{ads}$) versus T (Figure 4) gave the heat of adsorption ($\Delta H°_{ads}$) and the entropy ($\Delta S°_{ads}$) according to the thermodynamic basic equation 5:

$$\Delta G°_{ads} = \Delta H°_{ads} - T \Delta S°_{ad} \qquad (5)$$

Table 5 clearly shows a good dependence of $\Delta G°_{ads}$ on T, indicating the good correlation among thermodynamic parameters. The negative value of $\Delta G°_{ads}$reflect that the adsorption of studied inhibitors on C-steel surface from 1 M HCl solution is spontaneous process and stability of the adsorbed layer on the carbon steel surface.

Generally, values of ΔG^{o}_{ads} around -20 kJ mol^{-1} or lower are consistent with the electrostatic interaction between the charged molecules and the charged metal (physical adsorption);those around -40 kJ mol-^{1} or higher involves charge sharing or transfer from organic molecules to the metal surface to form a coordinate type of bond (chemisorption) [24].From the obtained values of ΔG^{o}_{ads} it was found the existence of comprehensive physical and chemical adsorption)**.** The unshared electron pairs in sulphur, nitrogen may interact with d-orbitals of C-steel to provide a protective physical adsorbed film [25].
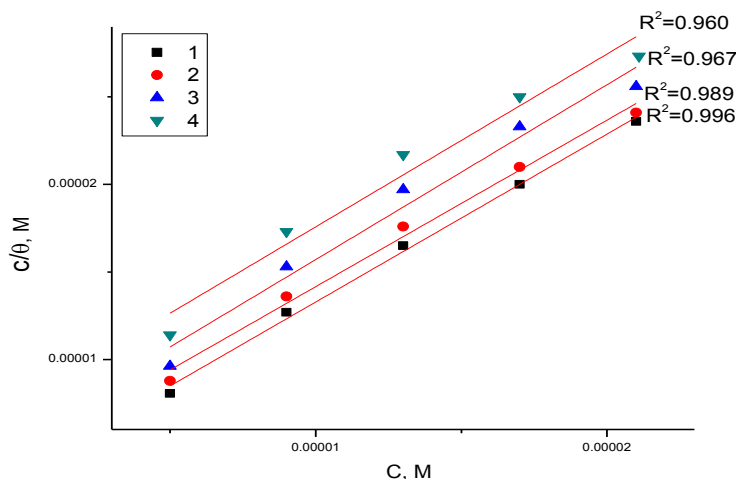

Figure 3. Langmuir adsorption isotherm of investigated inhibitors on C-steel surface in 1 M HCl at 25 ºC

Table 4. Equilibrium constant (K_{ads}) of investigated compounds adsorbed on C-steelsurface in 1M HCl at 25˚C

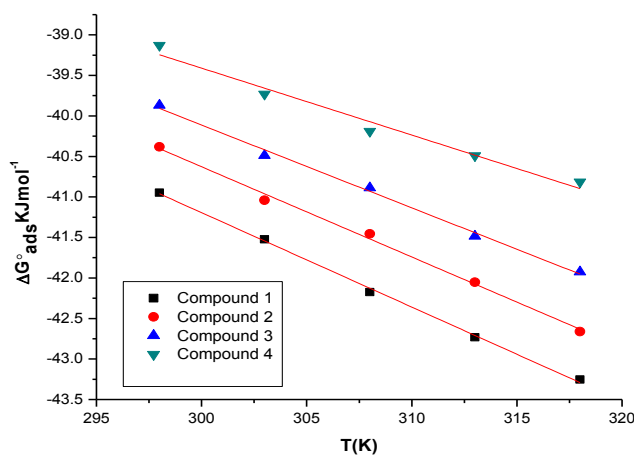| Temp ºC	1		2		3		4	
	$K_{ads} \times 10^{-3}$ M^{-1}	R^2	$K_{ads} \times 10^{-3}$ M^{-1}	R^2	$K_{ads} \times 10^{-3}$ M^{-1}	R^2	$K_{ads} \times 10^{-3}$ M^{-1}	R^2
25	27.038	0.996	21.531	0.989	17.492	0.967	12.983	0.959
30	25.870	0.993	21.365	0.983	17.153	0.968	12.706	0.963
35	25.530	0.994	19.288	0.985	15.456	0.971	11.768	0.965
40	24.328	0.991	18.727	0.971	15.055	0.965	10.282	0.954
45	23.891	0.985	18.290	0.960	13.841	0.972	9.095	0.941

Figure 4: Variation of ΔG^{o}_{ads} versus T for the adsorption of inhibitors on C-steel surface in 1 M HCl at different temperatures

The values of thermodynamic parameter for the adsorption of inhibitors Table 5 can provide valuable information about the mechanism of corrosion inhibition.Endothermic adsorption process ($\Delta H^o_{ads} > 0$) is attributed unequivocally to chemisorption [26], an exothermic adsorption process ($\Delta H^o_{ads} < 0$) may involve either physisorption or chemisorption or mixture of both processes. In the presented case, the calculated values of ΔH°_{ads} for the adsorption of inhibitors in 1 M HCl indicating that these inhibitors may be mixture of both physical and chemical adsorption. The values of ΔS°_{ads} in the presence of inhibitors are large and negative that is accompanied with exothermic adsorption process. This indicates that an increase in disorder takes places on going from reactants to the metal-adsorbed reaction complex [27].

Table 5: Thermodynamic parameters for the adsorption of inhibitors on C-steel surface in 1MHCl at different temperatures

Inhibitor	Temperature °C	$K_{ads} \times 10^{-3}$ M^{-1}	$-\Delta G^o_{ads}$ kJ mol^{-1}	$-\Delta H^o_{ads}$ kJ mol^{-1}	$-\Delta S^\circ_{ads}$ J mol^{-1} K^{-1}
1	25	27.038	40.95		116.63
	30	25.870	41.52		116.61
	35	25.530	42.17	6.19	116.83
	40	24.328	42.73		116.75
	45	23.891	43.25		116.56
2	25	21.531	40.38		111.18
	30	21.365	41.04	7.25	111.52
	35	19.288	41.46		111.36
	40	18.727	42.05		111.19
	45	18.290	42.66		111.06
3	25	17.492	39.87		101.49
	30	17.153	40.49	9.65	101.77
	35	15.456	40.89		101.42
	40	15.055	41.48		101.71
	45	13.841	41.92		101.40
4	25	12.983	39.13		82.35
	30	12.706	39.73	14.63	82.85
	35	11.768	40.19		82.99
	40	10.282	40.49		82.63
	45	9.095	40.81		82.22

3.4 Kinetic –thermodynamic corrosion parameters
The effect of temperature on both corrosion and corrosion inhibition of carbon steel in 1 M HCl solution in the absence and presence of different concentrations of investigated compounds at different temperatures ranging from 25ºC to 45ºC was studied using weight loss measurements. The corrosion rate increases with increasing temperature both in uninhibited and inhibited acid. The apparent activation energy (E^*_a) for the corrosion process can be calculated from Arrhenius-type equation (6):

$$k_{corr} = A \exp(E^*_a/RT) \qquad (6)$$

where E^*_a is the apparent activation corrosion energy, R is the universal gas constant, T is the absolute temperature and A is the Arrhenius pre-exponential constant. Values of apparent activation energy of corrosion for C-steel in 1 M HCl(E^*_a = (slope) 2.303 x R) shown in Table 6, without and with various concentrations of compound (1) determined from the slope of log (k_{corr}) versus 1/T plots are shown in Figure 5. Inspection of the data shows that the activation energy is higher in the presence of inhibitors than in its absence. The alternative formulation of transition state equation is shown in Eq. (7):

$$k_{corr} = (RT/Nh)\exp(\Delta S^*/R)\exp(-\Delta H^*/RT) \qquad (7)$$

where $k_{corr}$is the rate of metal dissolution, h is Planck's constant, N is Avogadro's number, ΔS^* is the entropy of activation and ΔH^* is the enthalpy of activation. Figure 6shows a plot of log (k_{corr}/T) against (1/T) in the case of inhibitor (1) in 1 M HCl,similar behavior is observed in the case of other investigated inhibitors (not shown). Straight lines are obtained with a slopes equal to (ΔH^* /2.303R) and intercepts are [log (R/Nh + ΔS^*/2.303R)] are calculated Table 6.

Figure 5: Log k_{corr} vs. (1/T) curves for Arrhenius plots for C-steel corrosion rates (k_{corr}) after 240 minutes of immersion in 1M HCl $_{in}$ the absence and presence of various concentrations of inhibitor (1)
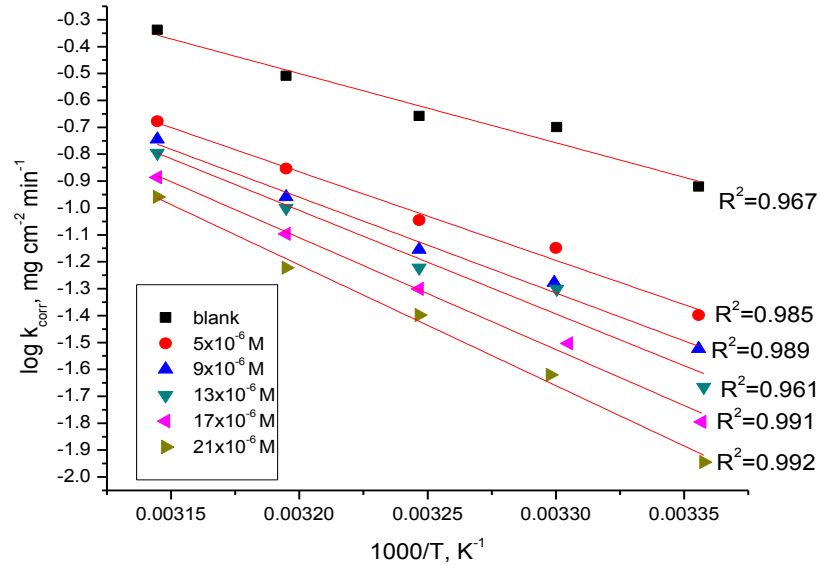

Figure 6. Log (k_{corr}/T) vs. (1/T) curves for Transition plots for C-steel corrosion rates (k_{corr}) after 240 minutesof immersion in 1M HCl in the absence and presence of various concentrations of inhibitor (1)
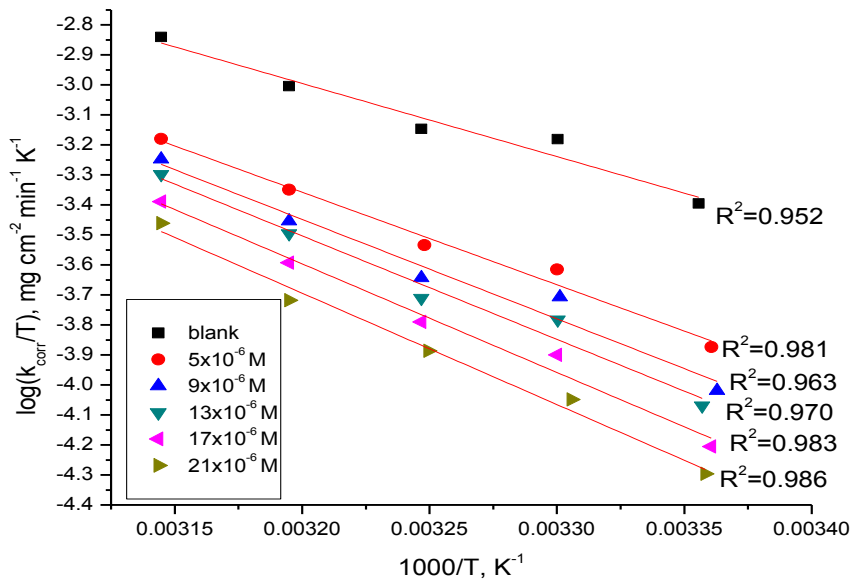
J. Mater. Environ. Sci. 6 (4) (2015) 1022-1039
ISSN: 2028-2508
CODEN: JMESCN

Fouda et al

The increase in E_a^* with increase inhibitor concentration Table 6 is typical of physical adsorption. The positive signs of the enthalpies (ΔH^*) reflect the endothermic nature of the brass dissolution process. Value of entropies (ΔS^*) imply that the activated complex at the rate determining step represents an association rather than a dissociation step, meaning that a decrease in disordering takes place on going from reactants to the activated complex [28].However, the value of (ΔS^*) decreases gradually with increasing inhibitor concentrations in all the acid media .

Table6.Activation parameters for C-steel corrosion in the absence and presence ofvarious concentrations of investigated compounds in 1M HCl solutions

Inhibitor	[inh]x10^{-6} M	E_a^* kJmol^{-1}	ΔH^* kJ mol^{-1}	$-\Delta S^*$ J mol^{-1}K^{-1}
Blank	0	49.2	46.7	105.5
1	5	63.0	59.1	72.7
	9	68.2	65.5	60.4
	13	73.7	68.1	53.2
	17	75.7	70.3	44.5
	21	78.0	76.6	40.7
2	5	59.5	56.5	89.5
	9	64.6	60.8	83.3
	13	69.8	66.1	76.8
	17	74.3	70.8	71.9
	21	78.3	77.5	68.0
3	5	55.7	52.0	93.6
	9	60.0	57.2	89.8
	13	63.4	59.8	83.4
	17	68.5	65.0	75.6
	21	73.1	70.9	71.4
4	5	52.4	48.8	102.5
	9	57.7	55.9	97.8
	13	61.7	58.5	90.7
	17	65.5	63.2	86.5
	21	70.3	67.6	81.7

3.5 Potentiodynamic Polarization Measurements

Figure 7 shows typical polarization curves for C-steel in 1 M HCl media. Various corrosion parameters such as corrosion potential ($E_{corr.}$), anodic and cathodic Tafel slopes (β_a, β_c), the corrosion current density (i_{corr}), the degree of surface coverage (θ) and the inhibition efficiency (%IE) are given in Table 7. It can see from the experimental results that in all cases, addition of inhibitors induced a significant decrease in cathode and anodic currents. The values of E_{corr} were affected and slightly changed by the addition of inhibitors. This indicates that these inhibitors act as mixed-type inhibitors. The slopes of anodic and cathodic Tafel lines (β_a and β_c), were slightly changed (Tafel lines are parallel), on increasing the concentration of the tested compounds which indicates that there is no change of the mechanism of inhibition in the presence and absence of inhibitors. The order of inhibition efficiency of investigated inhibitors at different concentrations are: 1 > 2 > 3 > 4(Table7). The results are in good agreement with those obtained from weight-loss measurements.
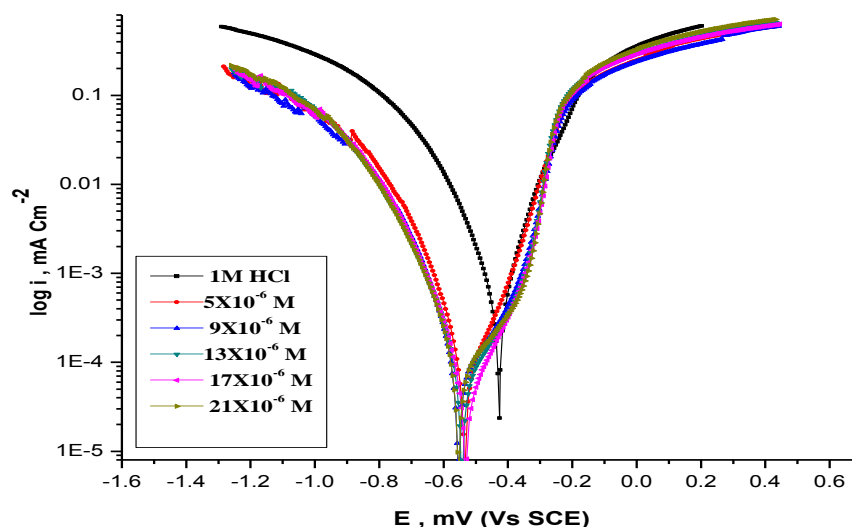
Figure 7. Potentiodynamic polarization curves for the dissolution of C-steel in 1M HCl in the absence and presence of different concentrations of inhibitor (1) at 25 °C

Table 7. Corrosion potential (E_{corr}), corrosion current density (i_{corr}), Tafel slopes (β_c, β_a), degree of surface coverage (θ), and inhibition efficiency (% IE) of C-steel in 1M HCl at 25°C for investigated compounds

Inh.	$[inh] \times 10^{-6}$ M	$-E_{corr}$ mV vs SCE	$i_{corr} \times 10^{-4}$ $\mu A\ cm^{-2}$	β_a mV dec^{-1}	β_c mV dec^{-1}	C. R mpy	Θ	% IE
Blank	0	428	553.1	1042	128.80	252.90	-----	-----
1	5	534	112.2	157	111.4	51.38	0.797	79.7
	9	554	98.5	215	109.1	45.01	0.822	82.2
	13	542	68.8	174	103.80	31.46	0.876	87.6
	17	543	53.6	151	101.50	24.49	0.903	90.3
	21	553	37.7	137	83.60	17.2	0.932	93.2
2	5	505	121.1	202	135.1	55.23	0.780	78.0
	9	544	111.2	163	122.1	50.79	0.802	80.2
	13	532	88.7	144	101.50	40.54	0.840	84.0
	17	522	76.1	134	103.30	34.75	0.862	86.2
	21	524	50.2	119.8	92.90	23.1	0.909	90.9
3	5	506	144.0	167.1	131.20	65.99	0.740	74.0
	9	517	130.2	168.4	124.20	59.38	0.765	76.5
	13	512	116.3	172.8	121.50	52.85	0.790	79.0
	17	522	89.5	165.7	123.80	40.92	0.838	83.8
	21	533	69.7	158.8	107.20	31.8	0.874	87.4
4	5	514	274.2	192.4	144.10	125.00	0.504	50.4
	9	514	252.1	174.7	139.70	115.20	0.544	54.4
	13	526	197.3	185.8	111.30	89.80	0.643	64.3
	17	503	172.2	172.7	120.20	78.80	0.689	68.9
	21	553	117.0	186.1	94.80	53.3	0.788	78.8

3.6. Electrochemical Impedance Spectroscopy (EIS) Measurements

EIS is well-established and it is powerful technique for studying the corrosion. Surface properties, electrode kinetics and mechanistic information can be obtained from impedance diagrams [29]. Figure10shows the Nyquist(a) and Bode(b) plots obtained at open-circuit potential both in the absence and presence of increasing concentrations of investigated compounds at 25°C. The increase in the size of the capacitive loop with the addition of investigated compounds shows that a barrier gradually forms on the C-steel surface. The increase in the capacitive loop size (Figure 10a) enhances, at a fixed inhibitor concentration, following the order: 1 > 2 > 3 > 4, confirming the highest inhibitive influence of compound (1). Bode plots (Figure 10b), show that the total impedance increases with increasing inhibitor concentration (log Z vs. log f). But (log f vs. phase), also Bode plot shows the continuous increase in the phase angle shift, obviously correlating with the increase of inhibitor adsorbed on C-steel surface. The Nyquist plots do not yield perfect semicircles as expected from the theory of EIS. The deviation from ideal semicircle was generally attributed to the frequency dispersion [30]as well as to the inhomogenities of the surface.
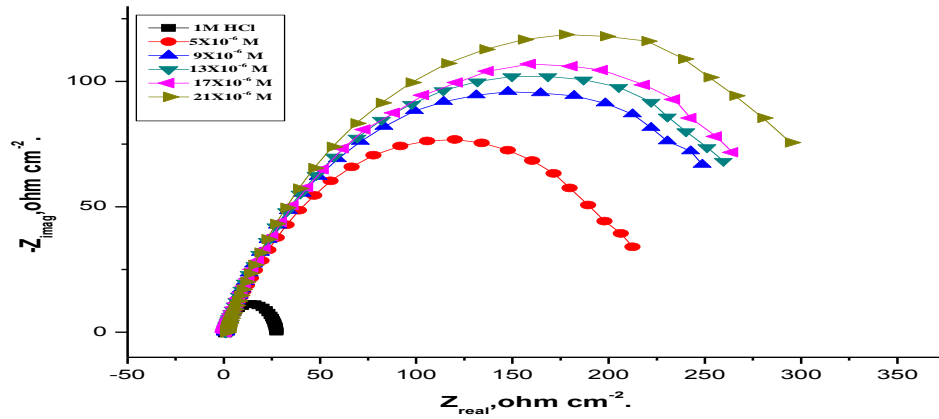

Figure 9a. The Nyquist plots for the corrosion of C-steel in 1M HCl in the absence and presence of different concentrations of inhibitor (1) at 25° C
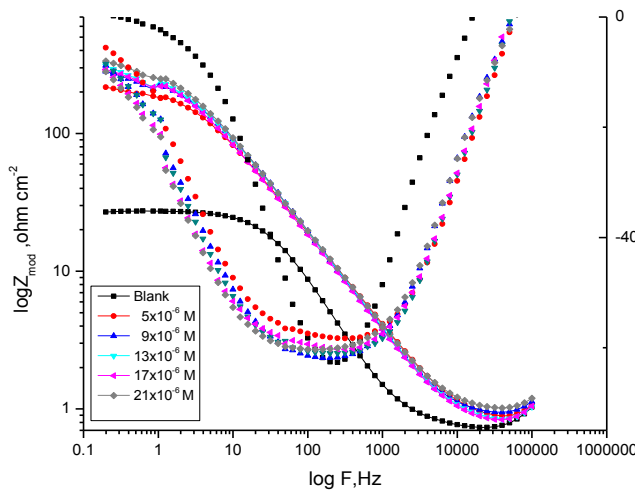

Figure 9b. The Bode plots for the corrosion of C-steel in 1M HCl in the absence and presence of different concentrations of inhibitor (1) at 25°C
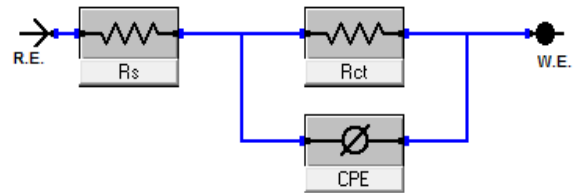
Figure 8. Equivalent circuit model used to fit experimental EIS

EIS spectra of the investigated compounds were analyzed using the equivalent circuit, Figure 8, which represents a single charge transfer reaction and fits well with our experimental results. The constant phase element, CPE, is introduced in the circuit instead of a pure double layer capacitor to give a more accurate fit [31].The double layer capacitance, C_{dl}, for a circuit including a CPE parameter (Y0 and n) were calculated from eq.14 [32]:

$$Cdl = Y_0(\omega_{max})^{n-1} (8)$$

where Y_0 is the magnitude of the CPE, $\omega_{max} = 2\pi f_{max}$, f_{max} is the frequency at which the imaginary component of the impedance is maximal and the factor n is an adjustable parameter that usually lies between 0.50 and 1.0. After analyzing the shape of the Nyquist plots, it is concluded that the curves approximated by a single capacitive semicircles, showing that the corrosion process was mainly charged-transfer controlled [33,34] .The general shape of the curves is very similar for all samples (in presence or absence of inhibitors at different immersion times) indicating that no change in the corrosion mechanism [35].From the impedance data Table 8, we concluded that the value of R_{ct} increases with increasing the concentration of the inhibitors and this indicates an increase in % IE_{EIS}, which in concord with the EFM results obtained.

Table 8. Electrochemical kinetic parameters obtained by EIS technique for in 1 M HCl without and with various concentrations of investigated compounds at 25^oC

Concentration, M		R_p, $k\Omega$ cm^2	C_{dl}, μF cm^{-2}	θ	% IE
1 M HCl		26.5	330	---	---
1	$5x 10^{-6}$	178.6	155	0.875	87.5
	$9x 10^{-6}$	249.5	150	0.901	90.1
	$13x 10^{-6}$	276.1	137	0.907	90.7
	$17x 10^{-6}$	288.1	130	0.913	91.3
	$21x 10^{-6}$	323.7	41	0.921	92.1
2	$5x 10^{-6}$	212.4	229	0.852	85.2
	$9x 10^{-6}$	266.2	213	0.894	89.4
	$13x 10^{-6}$	284.5	197	0.904	90.4
	$17x 10^{-6}$	303.3	192	0.908	90.8
	$21x 10^{-6}$	333.1	187	0.918	91.8
3	$5x 10^{-6}$	132.9	265	0.801	80.1
	$9x 10^{-6}$	159.1	241	0.834	83.4
	$13x 10^{-6}$	177.6	223	0.851	85.1
	$17x 10^{-6}$	257.5	221	0.898	89.8
	$21x 10^{-6}$	298.1	205	0.909	90.9
4	$5x 10^{-6}$	62.92	319	0.580	58
	$9x 10^{-6}$	67.5	276	0.608	60.8
	$13x 10^{-6}$	79.08	244	0.666	66.6
	$17x 10^{-6}$	98.6	237	0.732	73.2
	$21x 10^{-6}$	119	215	0.781	78.1

In fact the presence of inhibitors enhances the value of R_{ct} in acidic solution. Values of double layer capacitance are also brought down to the maximum extent in the presence of inhibitor and the decrease in the values of CPE follows the order similar to that obtained for i_{corr} in this study. The decrease in CPE/C_{dl} results from a decrease in local dielectric constant and/or an increase in the thickness of the double layer, suggesting that organic derivatives inhibit the C-steel corrosion by adsorption at metal/acid [36,37] .The inhibition efficiency was calculated from the charge transfer resistance data from Eq.9[38]:

$$\% IE_{EIS} = [1 - (R^\circ_{ct}/ R_{ct})] \times 100 \qquad (9)$$

where R^o_{ct} and Rct are the charge-transfer resistance values without and with inhibitor respectively.

3.7. Electrochemical Frequency Modulation Measurements

EFM is a nondestructive corrosion measurement technique that can directly and quickly determine the corrosion current values without prior knowledge of Tafel slopes, and with only a small polarizing signal. These advantages of EFM technique make it an ideal candidate for online corrosion monitoring [39]. The great strength of the EFM is the causality factors which serve as an internal check on the validity of EFM measurement. The causality factors CF-2 and CF-3 are calculated from the frequency spectrum of the current responses. Figure 10 shows the EFM Intermodulation spectra (current vs frequency) of C-steel in HCl solution containing different concentrations of compound (1). Similar curves were obtained for other compounds (not shown). The harmonic and intermodulation peaks are clearly visible and are much larger than the background noise. The two large peaks, with amplitude of about 200 μA, are the response to the 40 and 100 mHz (2 and 5 Hz) excitation frequencies. It is important to note that between the peaks there is nearly no current response (<100 nA). The experimental EFM data were treated using two different models: complete diffusion control of the cathodic reaction and the "activation" model. For the latter, a set of three non-linear equations had been solved, assuming that the corrosion potential does not change due to the polarization of the working electrode[40].The larger peaks were used to calculate the corrosion current density (i_{corr}), the Tafel slopes (β_c and β_a) and the causality factors (CF-2 and CF-3).These electrochemical parameters were listed in Table 9.

Table 9. Electrochemical kinetic parameters obtained from EFM technique for C-steel in 1M HCl in the absence and presence of different concentrations of compounds

Inh.	Conc., $\times 10^6$M	i_{corr} uA cm^{-2}	$\beta_{a,}$ mV dec^{-1}	β_c mVdec^{-1}	CF-2	CF-3	C. R, mpy	% IE
blank	0.0	426.4	53.2	58.47	1.20	2.79	194.8	-------
1	5	106.8	89.8	121.5	1.94	2.32	48.9	75.0
	9	86.58	89.5	126.9	2.00	1.21	39.6	79.7
	13	77.73	89.5	134.8	1.96	3.10	35.5	81.8
	17	74.58	94.8	136.6	1.91	2.87	34.1	82.5
	21	61.99	86.9	129.6	2.05	2.52	28.3	85.5
2	5	110.1	87.4	112.1	1.96	2.79	50.3	74.2
	9	93.95	91.9	167.7	2.00	2.60	42.8	78.0
	13	84.9	90.4	145.2	2.03	1.21	38.8	80.1
	17	76.06	89.6	158.5	1.96	1.16	34.8	82.2
	21	74.01	82.2	150.5	1.99	1.94	33.8	83.1
3	5	165.1	90.2	103.3	2.02	2.69	75.4	61.3
	9	156.7	82.1	110.3	2.05	3.70	71.6	63.3
	13	147.5	94.7	112.4	2.29	2.31	67.4	65.4
	17	119.4	85.6	104.3	1.91	2.84	54.6	72.0
	21	85.11	84.5	128.6	1.92	2.95	38.9	80.0
4	5	269.6	83.5	93.21	1.20	2.79	123.2	36.8
	9	239.4	88.6	92.04	2.45	1.92	109.4	43.9
	13	218.8	91.9	96.3	1.64	2.85	100.0	48.7
	17	179.6	86.2	116.9	1.87	1.61	82.1	57.9
	21	126.3	104.0	122.9	1.91	1.89	57.6	70.4

The data presented in Table 9 obviously show that, the addition of any one of tested compounds at a given concentration to the acidic solution decreases the corrosion current density, indicating that these compounds inhibit the corrosion of C-steel in 1 M HCl through adsorption. The causality factors obtained under different experimentalconditions are approximately equal to the theoretical values (2 and 3) indicating that the measured data are verified and of good quality. The inhibition efficiencies %IE$_{EFM}$ increase by increasing the inhibitor concentrations and was calculated as from Eq. (10):

$$\%IE_{EFM} = [1-(i_{corr}/i^{o}_{corr})]\times100 \qquad (10)$$

where i^{o}_{corr} and i_{corr} are corrosion current densities in the absence and presence of inhibitor, respectively. The inhibition sufficiency obtained from this method is in the order: 1> 2 > 3> 4
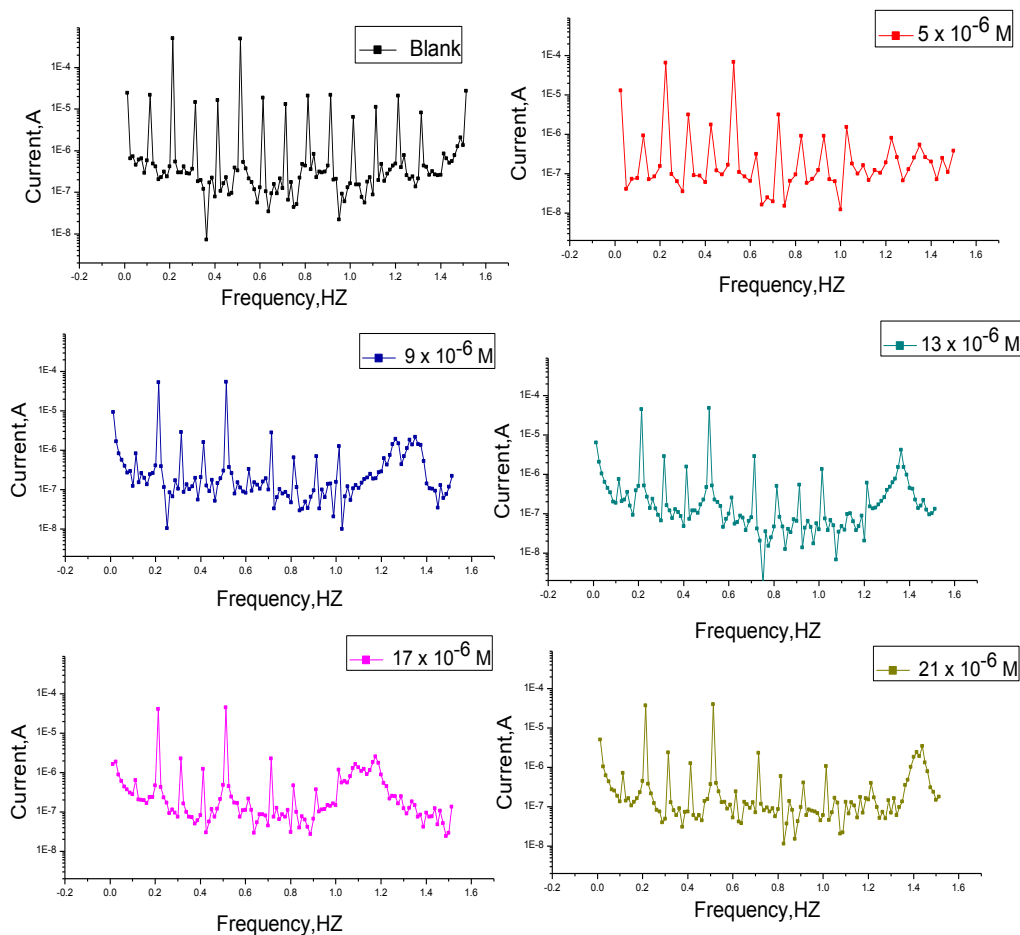

Figure 10. EFM spectra for C-steel in 1 M HClin the absence and presence of different concentrations of inhibitor (1) at 25 °

3.8. Surface Examinations

SEM and EDX experiments were carried out in order to verify if the investigated compounds are in fact adsorbed on C-steel surface or just peeled off the surface. SEMimages were indicative of the changes that accompany both corrosion and protection of the carbon steel surface (Fig. 11a–f).Figure 11a shows the free metal. Figure 11b shows the damage caused to the surface by hydrochloric acid. Figures 12c, d, e show SEM images of the carbon steel surface after treatment with 1 M HCl containing 21 x 10^{-6}M of investigated inhibitors. From these images, it is obvious that the steel surface seems to be almost unaffected by corrosion. This is because of adsorption of investigated inhibitors forming a thin protective film of the inhibitors on the metal surface. This film is responsible for the highly efficient inhibition by these inhibitors. The corresponding EDX profile analyses are presented in Table 8 and Figure 12 for investigated compounds not shown. It is also important to notice the existence of C, S and N peaks in the EDX spectra of the C-steel surface corresponding to the samples immersed for 24 hrs. in solutions containing the optimum concentration of these compounds. The formation of a thin inhibitor film is in agreement with the SEM observations.
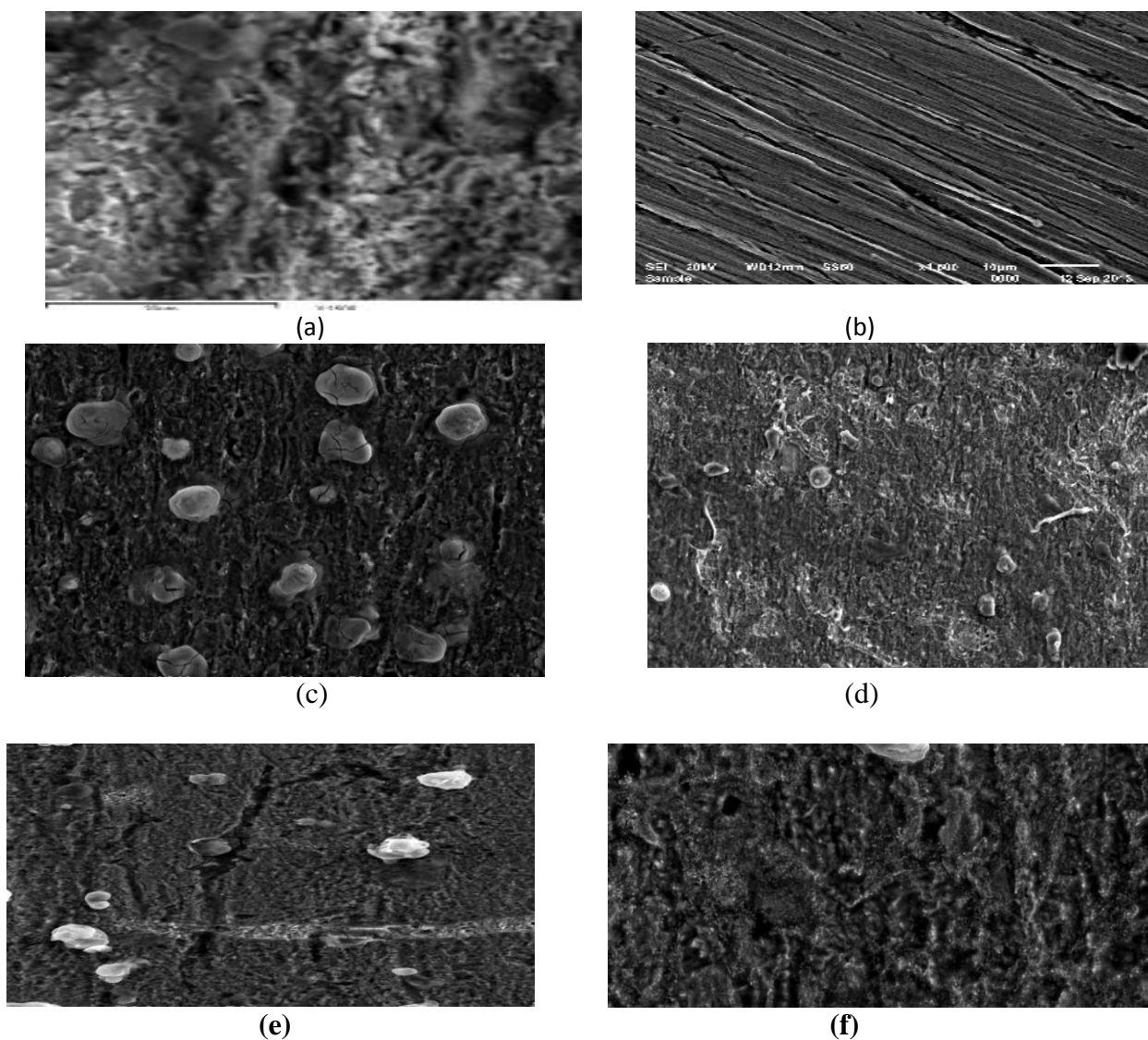
Figure 11: SEM micrographs of C-steel surface (a) before of immersion in 1 M HCl, (b) after 24 h of immersion in 1 M HCl , (c) after 24 h of immersion in 1 M HCl+ 21×10^{-6} M of compound 1,(d) after 24 h of immersion in 1 M HCl+ 21×10^{-6} M of compound 2 and (e) after 24 h of immersion in 1 M HCl+ 21×10^{-6} M of compound 3 and (f) after 24 h of immersion in 1 M HCl+ 21×10^{-6} M of compound 4 at 25°C

Table 10. Surface composition (weight %) of C-steel after 1 day of immersion in 1 M HCl + 21 x 10^{-6}M of investigated compounds

Mass %	C	Si	Mn	Fe	S	N
pure	11.59	0.38	0.76	87.72	---	----
Blank	16.66	0.26	0.74	82.06	---	----
1	13.25	0.49	0.49	60.29	22.33	3.92
2	11.46	0.27	0.45	61.5	21.67	3.21
3	9.70	0.26	0.43	61.28	18.24	2.81
4	8.99	0.19	0.37	62.02	17.64	1.90

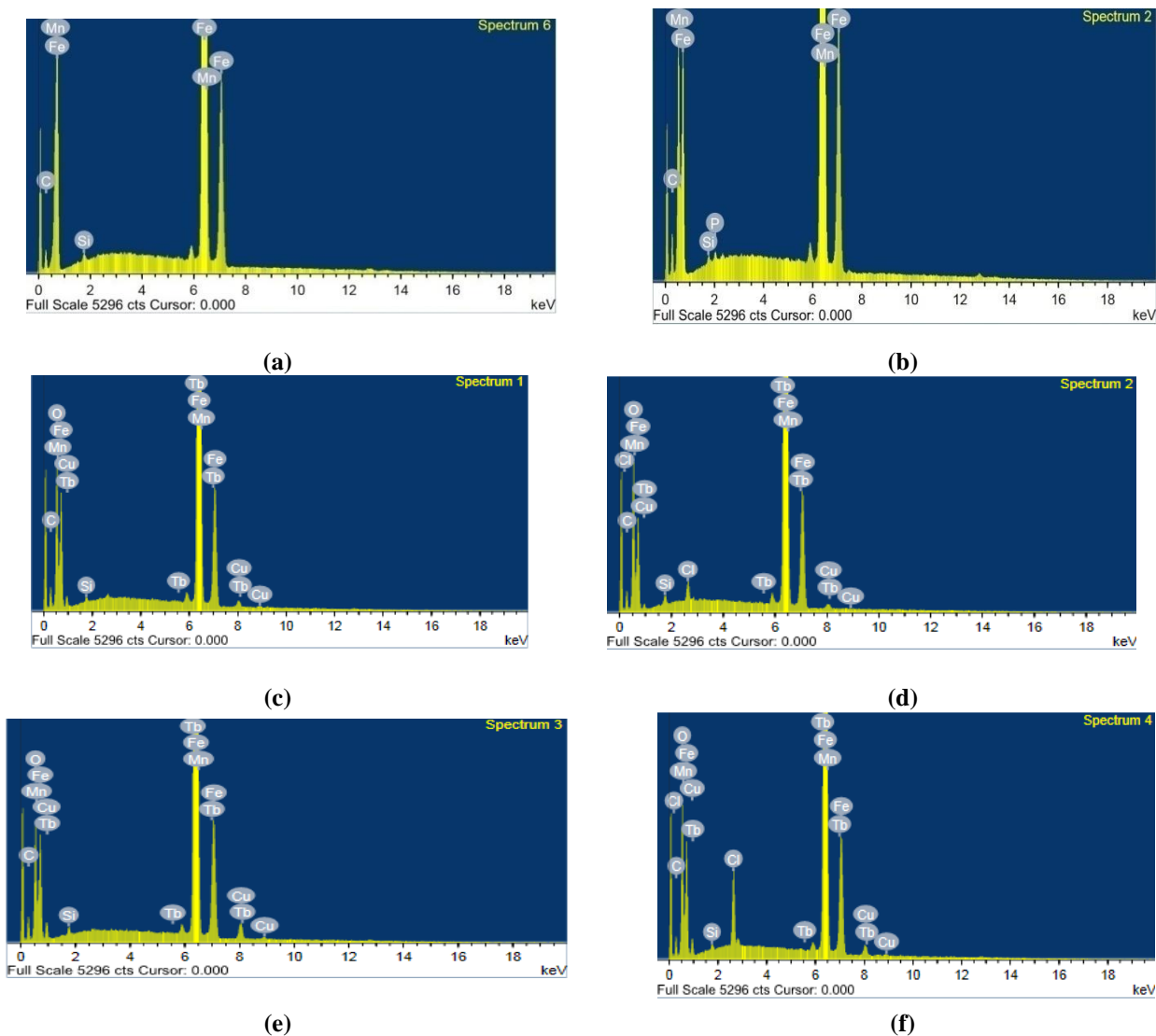**Figure 12**. EDX spectra of C-steel surface (a) before of immersion in 1 M HCl,(b) after24 h of immersion: in 1 M HCl, (c) in 1 M HCl+ 21×10^{-6} M compound 1, (d) in 1 M HCl+ 21×10^{-6} M compound 2 (e) in 1 M HCl+ 21×10^{-6}M compound 3 and (f) in 1 M HCl+ 21×10^{-6} M compound 4 at 25°C .

3.9. Quantum Chemical Calculations

The E_{HOMO} indicates the ability of the molecule to donate electrons to an appropriated acceptor with empty molecular orbitals, whereas the E_{LUMO} indicates its ability to accept electrons. The lower the values of E_{LUMO}, the more ability of the molecule is to accept electrons [41].The higher the values of E_{HOMO} of the inhibitor, the easier is its ability to offer electrons to the unoccupied d-orbital of metal surface, and the greater is its inhibition efficiency. As is seen from Table 10, compound (1) has the highest value of E_{HOMO}, which indicates that this molecule has high capacities of charge donation to the metallic surface and has highinhibition efficiency. It was found that the variation of the calculated LUMO energies among all investigated inhibitors is rule less, and the inhibition efficiency is misrelated to the changes of the E_{LUMO}Table 10.The HOMO–LUMO energy gap, ΔE approach, which is an important stability index, is applied to develop theoretical models for explaining the structure and conformation barriers in many molecular systems. The smaller the value of ΔE, the more is the probable inhibition efficiency the compound has [42--44]. It was shown from (Table 10) that compound(1) has the smallest HOMO–LUMO gap compared with the other molecules. Accordingly, it could be expected that compound(1) molecule has more inclination to adsorb on the metal surface than the other molecules.

There is a general consensus by several authors that the more negatively charged hetero atom is the more is its ability to adsorb on the metal surface through a donor–acceptor type reaction [45-47]. Variation in the inhibition efficiency of the inhibitors depends on the presence of electronegative O- and N- atoms as substituent in their molecular structure. The calculated charges of selected atoms are presented in Fig. 10.

Table 10: E_{HOMO}, E_{LUMO}, energy gap (ΔE) and molecular area for the different compounds as obtained (PM3) method in gas phas

parameters	1	2	3	4
- E_{HOMO}, eV	8.939	8.849	8.898	8.954
-E_{LUMO}, eV	1.035	0.798	0.807	0.758
ΔE, eV	7.904	8.051	8.091	8.207
Molecular Area, °A	119.958	187.545	141.738	111.417

3.10. Mechanism of Corrosion Inhibition
The inhibition mechanism involves the adsorption of the inhibitor on the metal surface immersed in aqueous HClsolution. Four types of adsorption [48]may takeplaceinvolving organic molecules at the metal–solution interface: 1)Electrostatic attraction between the charged molecules and the charged metal; 2) Interaction of unshared electron pairs in the molecule with the metal; 3) Interaction of π-electrons with the metal; 4) Combination of all the above. From the observations drawn from the different methods, corrosion inhibition of C-steel in 1M HCl solutions by the investigated inhibitors as indicated from weight loss, potentiodynamic polarization and EIS techniques were found to depend on the concentration and the nature of the inhibitor. The order of inhibition efficiency is as follows: 1>2>3>4
The thiadiazole derivatives of the studied compounds contain polar groups such as sulfur and nitrogen. Each atom is an adsorptioncenter and the inhibition efficiency depends on the electron density around thiscenter; higher the electron density at the adsorptioncenter, greater is the inhibition efficiency. The highest inhibition efficiency was observed for compound(1) as it has an additional sulfur atom with lone pair ofelectrons. These electrons interact with the vacant d-orbital of iron present in the C-steel surface and adsorb strongly, thereby blocking more number of adsorption sites on the C-steel surface.There is decrease in the IE of thiadiazole derivatives as the size of side chain alkyl group decreases. The presence of tertiary-butyl group in compound (2) also increases the density of electrons on sulphur and nitrogen atom caused by resonance effect, which facilitate stronger adsorption of compound(2) on the C-steel surface. This leads to higher IE of compound(2) than compound(3) compared with (4). The IE goes on decreasing with decrease in the number of carbon atoms as a consequence of the decrease in the electron density on N and S atoms. It has been previously reported in literature, that inhibiting effect depends mainly on inhibitor concentration, the molecular structure, size and structure of the side chain in the organic compounds. It is observed that, the inhibition efficiency of the thiadiazole derivatives increases with increase in concentration as a result of higher surface coverage in solutions containing higher concentration of inhibitors.

Conclusions
From the overall experimental results the following conclusions can be deduced:
1. The investigated compounds are good inhibitors and act as mixed type inhibitors for C-steel corrosion in 1 M HCl.
2. Reasonably good agreement was observed between the values of IE obtained by the weight loss and electrochemical measurements. The order of % IE of these investigated compounds is in the following order: 1 > 2 > 3 > 4.
3. The results obtained from all electrochemical measurements showed that the inhibiting action increases with the inhibitor concentration and decreases with raisingthe temperature.
4. Double layer capacitances decrease with respect to blank solution when the inhibitor is added. This fact confirms the adsorption of these molecules on the carbon steel surface.
5. The thermodynamic parameters revealed that the inhibition of corrosion by investigated compounds is due to the formation of a physical adsorbed film on the metal surface.
6. The adsorption of inhibitor on C-steel surface in HCl solution follows Langmuir isotherm for these compounds.
7. The negative values of $\Delta G°_{ads}$ indicate spontaneous adsorption of the inhibitors on the C-steel Surface
8. Quantum chemical parameters for these investigated compounds were calculated to provide further insight into the mechanism of inhibition of the corrosion process.

References

1. Huilong, W., Jiashen Z., and Jing, L., *Anti-Corros. Methods and Mater*. 49 (2002) 127
2. Said, M. T., Ali, S. A., and Rahman, S.U., *Anti-Corros. Methods and Materials*, 50(2003) 201
3. Atia, A., and Saleh, M. M., *J. Appl. Electrochem.,* 33(2003)171
4. Tamilselvi, S. and Rajeswari, S., *Anti-Corros. Methods and Materials*, 50 (2003) 223
5. Keera, S. T., *Anti-Corros. Methods and Materials*, 50(2003)280
6. Chetouani A., Hammouti B., Aouniti A, Benchat N., Benhadda T., *Prog. Org. Coat.* 45 (2002) 373.
7. Bekkouch K, Aouniti A, Hammouti B., KertitS., *J. Chim. Phys*. 96 (1999) 838.
8. Kertit S., Hammouti B., Taleb M. Brighli M., *Bull. Electrochem*. 13 (1997) 241.
9. Bouklah M., Benchat N., Aouniti A., Hammouti B., Benkaddaddour M., Lagrenee M. Vezine H., Bentiss F., *Prog. Org. Coat.* 51 (2004) 118.
10. Bentiss, F., Lagrenée, M., Traisnel, M. and Hornez, J. C., *Corros. Sci.,* 41(1999)789
11. Bentiss, F., Lagrenée, M. and Traisnel, M., *Corrosion*, 56(2000)733
12. Bentiss, F., Traisnel, M. and Lagrenée, M., *J. Appl. Electrochem*., 31 (2001) 41
13. Growcock, F. B. and Lopp, V. R., *Corros. Sci.,* 28(1988)397
14. Sherif E.M., Su-Moon Park, *Electrochim. Acta* 51(2006) 6556
15. Sherif E.M, *Appl. Surf. Sci.* 252 (2006) 8615
16. Sherif E.M, Su-Moon Park, *Corros. Sci.* 48 (2006) 4065
17. Sherif E.M, Shamy A.M., Ramla M. M., El Nazhawy A. O.H., *Mater. Chem. Phys*. 102 (2007) 231
18. Vastag Gy., Szöcs E., ShabanA., Kálmán E., *Pure Appl. Chem*. , 73 (2001) 1861
19. OguzieE. E., *Mater. Letters*, 59 (2005) 1076.
20. Khaled K. F., *Mater. Chem. Phys.,* 112 (2008) 290
21. Khaled K. F., *J. Appl. Electrochem*., 39 (2009) 429
22. Bosch R. W., Hubrecht J., Bogaerts W. F., Syrett B. C., *Corrosion* 57 (2001) 60.
23. Abdel–Rehim S. S., Khaled K. F., Abd–Elshafi N. S., *Electrochim. Acta* 51 (2006) 3269
24. Lorenz, W. J., Mansfeld F., Corros. *Sci.,* 21(1981)647
25. Yurt A, Bereket G, Kivrak A, Balaban A & Erk B, *J Appl Electrochem*, 35 (2005) 1025.
26. Bentiss F, Traisnel M & Lagrenee M, *Corros Sci.,* 42 (2000) 127.
27. Durnie W, Marco R D, Jefferson A & Kinsella B, *J Electrochem Soc,* 146 (1999) 1751.
28. Aksut, A. A., Lorenz, W. J. L. and Mansfeld, F., *Corros.Sci.* 22(1982)611
29. Lorenz W. J., Mansfeld F., *Corros. Sci.* 21 (1981) 647.
30. El Achouri M., Kertit S., Gouttaya H.M., Nciri B., Bensouda Y., Perez L., Infante M.R., Elkacemi K., *Prog. Org. Coat*., 43 (2001) 267.
31. Macdonald J.R., Johanson W.B., in: J.R. Macdonald (Ed.), Theory in Impedance Spectroscopy, John Wiley& Sons, New York, 1987.
32. Mertens S. F., Xhoffer C., Decooman B. C., E. Temmerman, *Corrosion,* 53 (1997) 381.
33. Trabanelli G., Montecelli C., Grassi V., Frignani A., *J. Cem. Concr. Res.,* 35 (2005) 1804.
34. Trowsdate A. J., Noble B., Haris S.J., Gibbins I.S. R., Thomson G. E., Wood G. C., *Corros. Sci.,* 38 (1996) 177.
35. Reis F. M., De Melo H.G. and Costa I., *Electrochim. Acta*, 51 (2006) 17.
36. Lagrenee M., Mernari B., Bouanis M., Traisnel M., Bentiss F., *Corros. Sci.,* 44 (2002) 573.
37. McCafferty E., Hackerman N., *J. Electrochem. Soc.,* 119 (1972) 146.
38. Ma H., Chen S., Niu L., Zhao S., Li S., Li D., *J. Appl. Electrochem*, 32 (2002) 65.
39. Kus E., Mansfeld F., *Corros. Sci.* 48 (2006) 965.
40. Caigman G. A., Metcalf S. K., Holt E. M., *J. Chem. Cryst,* 30 (2000) 415.
41. Gao, G. and Liang, C. *Electrochim. Acta,* 52 (2007) 4554.
42. Feng, Y., Chen, S., Guo, Q., Zhang, Y., Liu, G., *J. Electroanal. Chem*. 602 (2007) 115.
43. Gece, G., Bilgic, S., *Corros. Sci*. 51 (2009) 1876.
44. Martınez, S., *Mater. Chem. Phys*. 77 (2002) 97.
45. Bereket, G., Ogretic, C., Ozsahim, C., *J. Mol. Struct. (THEOCHEM)* 663 (2003) 39.
46. Li, W., He, Q., Pei, C., Hou, B., *Electrochim. Acta* 52 (2007) 6386.
47. Rajenran, S., *J. Electrochem. Soc.* 54 (2005) 61
48. Schweinsberg D. P., Graeme A., George, Nanayakkara A.K. and Steinert D.A., *Corros. Sci.,* 28 (1988) Page.

(2015) ; http://www.jmaterenvironsci.com